

An Effective Method for early Diagnosis of Alzheimer Disease using Angular Radial Transform and Orthogonal Fourier Mellin Moments

R. Upneja^{1*}, A. Prashar²

^{1*} Dept. of Mathematics, Sri Guru Granth Sahib World University, Fatehgarh Sahib, India

¹Visiting Professor, Dept. of Electrical and Computer Engineering, University of Manitoba, Winnipeg, Canada

²Dept. of Mathematics, Sri Guru Granth Sahib World University, Fatehgarh Sahib, India

*Corresponding Author: prashar77@yahoo.com, Tel.: +91-98552-97007

Available online at: www.ijcseonline.org

Received: 15/Sep/2017, Revised: 28/Sep/2017, Accepted: 19/Oct/2017, Published: 30/Oct/2017

Abstract— Alzheimer's disease (AD) is a progressive neurodegenerative disorder dementia. The main challenges for medical investigators have been the early diagnosis of patients with AD because an early diagnosis can provide greater opportunities for patients to be eligible for more clinical trials. The transitional state between healthy control (HC) and AD with mild memory problems is Mild cognitive impairment (MCI). A reliable diagnosis of MCI can be very effective for early diagnosis of AD. In this study, a fast and accurate method based on rotation invariant descriptors is proposed and moments are used to distinguish the patients with AD and MCI from normal participants (HC) using structural Magnetic Resonance Images (MRI). The rotation invariant descriptors are among the best region based shape descriptors which are used in many medical image processing applications. The angular radial transform (ART) is one such rotation invariant descriptors. This descriptor has two essential characteristics as compared to moment based descriptors, viz., it has low computation cost and provides a large number of numerically stable features. However, its kernel consists of the sinusoidal functions which still needs high computation time. In this paper, we developed fast and effective method to compute the radial & angular sinusoidal functions using 8-way symmetry and also used fast & recursive method to extract the features from MRI images using OFMMs. These methods are used not only for binary images but for gray level images also. The proposed method is not only fast but also more reliable and numerically stable.

Keywords— Alzheimer, Early Diagnosis, Rotation Invariant Descriptors, Angular Radial Transform, Mild cognitive impairment, Healthy control, Orthogonal Fourier Mellin Moments, Zernike Moments.

I. INTRODUCTION

Alzheimer disease (AD) is a degenerative brain disease and the most common cause of dementia (Wilson et al., 2012; Barker et al., 2002). It is a slow degenerative disease with different evolution on every individual, but usually starting with mild memory problems and turning to severe brain damage in several years. An accurate and fast diagnosis at the early stage of Alzheimer (Lopez et al., 2009) plays an important role for the patients' medical treatment. It is associated with impaired consciousness and memory loss, and generally occurs in those people who aged over 65 (Brookmeyer et al., 1998). This disease was first described by German psychiatrist Alois Alzheimer in 1906 (Berchtold and Cotman, 1998). AD patients start experiencing cognitive impairments but not in a long period of time as they lose the spatio-temporal sense and are unable to recognize very familiar things or persons. AD has been increasing rapidly each year throughout the world. Since, currently there is no known cure for the AD, the early

diagnosis may help to slow down the rapid advance of this disease. According to the literature, pathological manifestation of AD begins many years before and it can be diagnosed using cognitive tests and MCI (a prodrome of AD) are expected to convert to probable AD at an annual rate of 10–15%, whereas healthy controls develop dementia at an annual rate of 1–2% (Johnson et al., 2006; Thompson and Apostolova, 2007; Whitwell et al., 2007; Grundman et al., 2004; Bischof et al., 2002). Due to its very mild cognitive impairment symptoms, MCI is more difficult to diagnose. In recent years, several techniques have been used for the classifications of AD and MCI individuals. Several attempts have been made by the researchers to prove & compare the efficiency and reliability of these techniques which include, Magnetic Resonance Imaging (MRI), Computed Tomography (CT), functional Magnetic Resonance Imaging (fMRI), Positron Emission Tomography (PET), and Single-photon Emission Computed Tomography (SPECT) (Erkinjuntti et al., 1989; Toyama et al., 2005; Davatzikos et al., 2008; Chaves et al., 2009; Cuignet et al., 2011; Magnin et al., 2009). A recent study demonstrated that classification

methods are capable of identifying AD patients via their MRI scans and achieved accuracy comparable to that obtained by experienced neuroradiologists (Kloppel et al., 2008). Many proposed techniques for diagnosing and classifying the AD, MCI & HC groups were based on grey matter (GM), white matter (WM), cerebrospinal fluid (CSF), Anatomical analysis by Freesurfer, Hippocampus Segmentation & Partial least squares (Cuignet et al., 2011; Magnin et al., 2009; Kloppel et al., 2008; Shen et al., 2013; Wang et al., 2013; Yang et al., 2013; Escudero et al., 2011; Colliot et al., 2008; Vinitha C. et al., 2014). Recently, Gorji and Haddadnia (Gorji and Haddadnia, 2015) proposed a technique for the early diagnosis of AD and MCI based on Pseudo Zernike moments (PZMs) features from MR images. The method used for classification is based on neural network technique. However, the method is giving the satisfactory accuracy but the feature computation process from the images was less efficient, slow and very complex and moreover they used only 25% of the images for the testing phase which decreases the reliability of the results. In this paper, we propose a fast and effective technique using ART for early diagnosis of Alzheimer Disease. The angular radial transform (ART) (Kotoulas and Andreadis, 2008) belongs to a class of rotation invariant descriptors which are region based shape descriptors. The term transform with ART arises due to the fact that its radial basis functions are sinusoidal functions unlike the ZMs, whose radial basis functions are radial polynomials. Otherwise, the computational form of ART is similar to that of the moments. In addition to being rotation invariant, the transform and moments are based on integration operation and thus all pixels in the image contribute to moment coefficients and hence they are robust to image noise. Two of the most important characteristics of ART which distinguishes it from the moments are: it is computationally fast and the high order transforms do not suffer from numerical instability unlike ZMs. These two important characteristics of the ART make it very useful in applications where large databases are used for image matching & retrieval of images and it requires a large size of feature vector. Due to this feature of the ART, MPEG-7 has adopted it as a region based descriptor (Bober, 2001). Although ART is computationally more efficient than moments & its derivation still requires the computation of sinusoidal terms present in its kernel functions. Since the computation of sinusoidal terms is time consuming & speed enhancement can be an important requirement in many applications involving on systems with low computation power. As angular radial transform is one of the most effective region based shape descriptors (Amanatiads et al., 2011) with better speed performance but its fast computation is still an important issue. There are two approaches in the literature (Hwang and Kim, 2006; Kotoule and Andreadis, 2008) which are very useful in the fast calculation of the ART. The method of (Hwang and Kim, 2006) uses 4-way symmetry/ anti-symmetry property of the radial and angular

functions and the method suggested by (Kotoule and Andreadis, 2008) is applicable to binary images only. In this paper, we derive a fast approach for the computation of ART on gray level images by proposing three strategies. We propose three recursive algorithms- the first for radial harmonic, the second for the angular harmonic & an 8-way symmetry/ anti-symmetry property is used for the radial and angular components. In doing so, only one octant of an image is considered for the computation & 8-way symmetry/ anti-symmetry results in the clustering of image pixels, which further enhances the speed of computation.

For many years, moments have been used as descriptors for the properties of the images in pattern recognition and therefore used them in many applications. Pattern recognition is used in number of image processing applications such as face recognition, fingerprint recognition, character recognition etc. There are different radial moment-based methods which can identify a pattern in terms of certain features. Some of the radial moments are like ZMs, PZMs, and OFMMs. There are many radial moments which are orthogonal and OFMMs is one of them. These moments are better in comparison with other moments as they store less redundant information. OFMMs are better in comparison to ZMs and PZMs, especially in terms of signal to noise ratio and reconstruction errors at low orders (Sheng and Shen, 1994). The performance of OFMMs is better due to its characteristics of possessing more number of zeros of radial polynomials as compared with ZMs & PZMs for the same order of moment. Moreover OFMMs have good reconstruction capability at low value of order. They found that OFMMs have better performance than ZMs in terms of pattern description and noise sensitivity. OFMMs can be worked with all sized images which may not be true with ZMs (Sheng and Shen, 1994). So we used fast and recursive technique of OFMMs for the early detection of Alzheimer's disease (Walia et al., 2012). Gorji & Haddadnia (Gorji and Haddadnia, 2015) presented a novel and efficient method based on PZMs for the diagnosis of MCI individuals from AD and HC groups using structural MR brain images. But they used ZMs instead of PZMs to extract the discriminative information from the MR images of the AD, MCI, and HC groups.

On the classification stage, various classifiers or similarity measures are examined to get the better accuracy rate of early diagnosis of AD & MCI. Alzheimer's disease Neuroimaging Initiative (ADNI) database (<http://www.loni.ucla.edu/ADNI>) is used for the experimental purpose. The ADNI was launched in 2003 by the National Institute on Aging (NIA), the National Institute of Biomedical Imaging and Bioengineering (NIBIB), the Food and Drug Administration (FDA), private pharmaceutical companies and non-profit organizations, as a \$60 million, 5-year public-private partnership. The primary goal of ADNI has been to test whether serial MRI, PET, other biological markers, clinical and neuropsychological

assessment can be combined to measure the progression of MCI and early AD. Determination of sensitive and specific markers of early AD progression is intended to aid researchers and clinicians to develop new treatments and monitor their effectiveness, as well as lessen the time and cost of clinical trials.

The work in this paper is organized by describing the basic formulation of ART in section 2. Section 3 describes the mathematical formulation of OFMMs followed by ZMs in section 4. In section 5, fast recursive relations for the radial & angular functions of the transform with their 8-way symmetry/anti-symmetry properties are discussed. Various classifiers (similarity measures) are discussed in section 6 followed by detailed experimental analysis in section 7. Section 8 consists the discussion about the proposed work followed by conclusion in Section 9.

II. ANGULAR RADIAL TRANSFORMS (ART)

The ART is a transform based region shape descriptor of MPEG-7 formally called Multimedia Content Description Interface (Bober, 2001). The ART coefficients of order n and repetition m for a continuous image function $f(x, y)$ ($f(x, y)$ gives intensity at position (x, y)) in a unit disk are defined by

$$A_{nm} = \iint_{x^2+y^2 \leq 1} V_{nm}^*(x, y) f(x, y) dx dy. \quad (1)$$

The function $V_{nm}^*(x, y)$ is the complex conjugate of the ART basis function $V_{nm}(x, y)$ defined by

$$V_{nm}(x, y) = \frac{1}{2\pi} R_n(r) e^{jm\theta}, \quad (2)$$

The radial part of the basis function is

$$R_n(r) = \begin{cases} 1, & n = 0 \\ 2 \cos(\pi n r), & n > 0, \end{cases} \quad (3)$$

where n is a non negative integer, m is an integer,

$$r = \sqrt{x^2 + y^2}, \quad j = \sqrt{-1} \quad \text{and} \quad \theta = \arctan\left(\frac{y}{x}\right).$$

In digital image processing the image function $f(x, y)$ is a discrete function defined in a rectangular coordinate system. Let (i, k) denote a pixel of an $N \times N$ image, then i represents its row position and k its column. The square domain $N \times N$ is mapped into a unit circle lying within the square $[-1, +1] \times [-1, +1]$ using the following transformation

$$x_i = \frac{2i+1-N}{N}, \quad y_k = \frac{2k+1-N}{N}, \quad i, k = 0, 1, \dots, N-1.$$

There is no analytical solution to the double integration involved in equation (1). Therefore, usually a zeroth order approximation is adopted to compute ART coefficients

$$A_{nm} = \frac{1}{2\pi} \sum_{x=0}^{N-1} \sum_{\substack{y=0 \\ x_i^2+y_k^2 \leq 1}}^{N-1} f(x, y) R_n(r) e^{-jm\theta} \Delta x \Delta y, \quad (4)$$

where

$$\Delta x_i = \Delta y_k = \Delta = \frac{2}{N}, \quad i, k = 0, 1, 2, \dots, N-1.$$

The ART is a complex function and can be expressed in terms of its real and imaginary parts, A_{nm}^R and A_{nm}^I , respectively, as given

$$A_{nm} = A_{nm}^R + jA_{nm}^I = \frac{2}{\pi N^2} \sum_{x=0}^{N-1} \sum_{\substack{y=0 \\ x_i^2+y_k^2 \leq 1}}^{N-1} f(x, y) R_n(r) (\cos(m\theta) - j \sin(m\theta)), \quad (5)$$

$$\text{where } r_{ik} = \sqrt{x_i^2 + y_k^2} \quad \text{and} \quad \theta_{ik} = \arctan\left(\frac{y_k}{x_i}\right).$$

III. ORTHOGONAL FOURIER-MELLIN MOMENTS (OFMMs)

Orthogonal Fourier Mellin moments have better performance than ZMs and PZMs in terms of image description and noise sensitivity in case of small images. For an image function $f(x, y)$ ($f(x, y)$ gives intensity at position (x, y)) the two dimensional OFMMs of order n with repetition m is given by

$$O_{nm} = \frac{n+1}{\pi} \iint_{x^2+y^2 \leq 1} f(x, y) V_{nm}^*(x, y) dx dy \quad (6)$$

where n is a non-negative integer, m is an integer (negative or positive) and $V_{nm}^*(x, y)$ is the complex conjugate of the moment basis function $V_{nm}(x, y)$ and the basis function $V_{nm}(x, y)$ is orthogonal to each other. It is defined as

$$V_{nm}(x, y) = R_{nm}^O(r) e^{jm\theta} \quad (7)$$

where $r = \sqrt{x^2 + y^2}$, $\theta = \tan^{-1}(y/x)$, $j = \sqrt{-1}$ and the radial polynomial $R_{nm}^O(r)$ is given by

$$R_{nm}^O(r) = \sum_{s=0}^n \frac{(-1)^{n+s} (n+s+1)! r^s}{s! (s+1)! (n-s)!} \quad (8)$$

Orthogonal Fourier Mellin Polynomials (OFMPs) are independent of m , therefore there is no restriction on m while computing OFMMs, unlike ZMs and PZMs. In fact, the Pseudo Zernike Polynomials (PZPs) become OFMPs for $m=0$. The angular function $e^{jm\theta}$ is computation intensive as

it involves the trigonometric functions. Walia (Walia et al., 2012) introduced a recursive approach for their computation without involving of trigonometric functions. The use of 8-way symmetry/anti-symmetry was first introduced by Hwang and Kim (Hwang and Kim, 2006).

IV. ZERNIKE MOMENTS

Zernike introduces a set of complex polynomials which form a complete orthogonal set over the interior of the unit circle, i.e. $x^2 + y^2 \leq 1$. The two dimensional Zernike moment of order n with repetition m over a unit disc is given by

$$Z_{nm} = \frac{n+1}{\pi} \iint_{x^2+y^2 \leq 1} f(x, y) V_{nm}^*(x, y) dx dy. \quad (9)$$

where

- n positive integer or zero
- m positive and negative integers subject to constraints
- $n - |m| = \text{even}, |n| \leq m$

The functions $V_{nm}^*(x, y)$ are the complex conjugate of Zernike polynomial $V_{nm}(x, y)$ which is orthogonal and complete. It is defined as

$$V_{nm}(x, y) = R_{nm}^Z(x, y) e^{jm\theta} \quad (10)$$

$$\theta = \tan^{-1}(y/x), \theta \in [0, 2\pi], j = \sqrt{-1}$$

Radial polynomial of ZMs is given by

$$R_{nm}^Z(x, y) = \sum_{s=0}^{(n-|m|)/2} \frac{(-1)^s (n-s)! (x^2+y^2)^{\frac{n-2s}{2}}}{s! \left(\frac{n+|m|}{2} - s\right)! \left(\frac{n-|m|}{2} - s\right)!} \quad (11)$$

Zernike moments with negative values of repetition m are obtained directly by making use of the complex conjugate of Zernike moments for positive values. The angular functions in ZMs can be computed using recursion without making use of trigonometric functions which are computation extensive and the 8-way symmetry/anti-symmetry properties of the kernel functions further reduces the time computation by factor 8 approximately (Singh and Upneja, 2012).

V. FAST COMPUTATION OF ART

At present, two methods exist for the fast computation of the ART. The first method suggested by Hwang and Kim (Hwang and Kim, 2006) uses 4-way symmetry for the computation of the radial function $R_n(r)$ and 4-way symmetry/anti symmetry property for the angular function $e^{jm\theta}$. The second method, proposed by Kotoulas and Andreadis (Kotoule and Andreadis, 2008), first approximates the radial and angular functions by least square

polynomials and computes the geometric moments of the image. The geometric moments are then used to compute the ART coefficients. The order of complexity is reduced from $O(N^2)$ to $O(N)$ but the method is applicable to only binary images because the approach which reduces the time complexity from $O(N^2)$ to $O(N)$ is not applicable to gray scale images. Our approach is based on the aspects, namely, the recurrence relations for the trigonometric functions and 8-way symmetry/ anti- symmetry of the radial & angular functions and this proposed method is used not only for binary images but also for gray level images.

5.1 Recurrence Relationship of the Trigonometric Functions

The trigonometric function $\cos(m\theta)$ and $\sin(m\theta)$ at a pixel location (i, k) can be computed using the recurrence relations given by the following steps (Sheng and Shen, 1994).

$$\text{Let } r_{ik} = (x_i^2 + y_k^2)^{1/2}, \quad a = \frac{x_i}{r_{ik}},$$

$$b = \frac{y_k}{r_{ik}}, \quad C_0 = \cos T[0] = 1.0 \quad \text{and}$$

$S_0 = \sin T[0] = 0.0$. The two tables $\cos T[]$ and $\sin T[]$ are used to save the trigonometric functions.

for $m=1$ to m_{\max}

$$C_m = aC_{m-1} - bS_{m-1}$$

$$S_m = aS_{m-1} + bC_{m-1}$$

$$\cos T[m] = C_m, \quad \sin T[m] = S_m$$

next m

The additional memory requirement is only $2(m_{\max} + 1)$ words

5.2 Recurrence Relation for the Calculation of the Angular Function, $\cos(n\pi r)$

The angular function $\cos(\pi nr)$ at pixel location (i, k) can be calculated recursively as given in section 5.1 with $a = \cos(\pi r_{ik})$ and $b = \sin(\pi r_{ik})$ and $\cos R[0] = 1$ and $\sin R[0] = 0$, where $\cos R[]$ and $\sin R[]$ are two variables used to save angular sinusoidal functions in the tabular form. This approach uses the library functions for the evaluation of $\cos(\pi r)$ and $\sin(\pi r)$ only for once, i.e. for $n=1$, and then uses the recurrence relations as given in section 5.1 for $n > 1$. The additional memory requirement is only $2(n_{\max} + 1)$ words.

5.3 Eight-way Symmetry/Anti Symmetry of the Kernel Functions

The 8-way symmetry/anti symmetry is very useful for the fast computation of the ART. Hwang and Kim (Hwang and Kim, 2006) use 4-way symmetry and observe significant reduction in the computation of the ART coefficients. Recently, Singh and Walia (Walia et al., 2012) use 8-way symmetry property in the Zernike moments calculation. We extend this property to the calculation of ART.

Let $P_1(x_i, y_k)$ be the coordinates of a pixel at location (i, k) , then $r_{ik} = \sqrt{x_i^2 + y_k^2}$ will be the same for all pixels with coordinates $(\pm x_i, \pm y_k)$ and $(\pm y_k, \pm x_i)$, where the eight symmetrical locations for a given point $P_1(x, y)$ are represented by the points P_2 through P_8 and the values of $\cos(m\theta_{ik})$ and $\sin(m\theta_{ik})$ at the 8 locations are determined according to the relationship table given in (Singh and Kaur, 2015). It is observed that from these tables, the values of $\cos(m\theta)$ and $\sin(m\theta)$ are calculated only once and these values are simply copied at the other seven locations. The 8-way symmetry reduces the number of computations from N^2 to $N(N+2)/8$ which is nearly one-eighth of its non symmetric counterpart.

VI. CLASSIFIERS (Similarity Measures)

Similarity measure is based on a distance measure and it is quite significant to the recognition and retrieval results. In order to retrieve or recognize most similar images to query image, similarity functions are computed between the query image and database images, which is based on a set of feature vectors.

Let x and y are two n -dimensional feature vectors of database and query image, then the various similarity measures are defined as:

The *Euclidean Distance* is given by:

$$d_{ed}(x, y) = \sqrt{\sum_{i=1}^n (x_i - y_i)^2} \quad (12)$$

The *Squared Chord* is given by:

$$d_{sc}(x, y) = \sum_{i=1}^n (\sqrt{x_i} - \sqrt{y_i})^2 \quad (13)$$

The *Chi-Square Distance* is given by:

$$d_{cs}(x, y) = \sum_{i=1}^n \frac{(x_i - y_i)^2}{x_i + y_i} \quad (14)$$

The *Extended Canberra Distance* is given by:

$$d_{ec}(x, y) = \sum_{i=1}^n \frac{|x_i - y_i|}{|x_i + u_x| + |y_i + u_y|} \quad (15)$$

$$\text{where } u_x = \sum_{i=1}^N x_i / n \quad u_y = \sum_{i=1}^N y_i / n$$

The *Cosine Measure Distance* is given by:

$$d_{cm}(x, y) = \frac{\sum_{i=1}^n x_i y_i}{\left(\sqrt{\sum_{i=1}^n x_i^2} \sqrt{\sum_{i=1}^n y_i^2} \right)} \quad (16)$$

The *Paper Similarity Measure Distance* is given by:

$$d_{ps}(x, y) = \left\| \frac{\sum_{i=1}^n x_i - \sum_{i=1}^n y_i}{1 + \sum_{i=1}^n x_i + \sum_{i=1}^n y_i} \right\| \quad (17)$$

The *Histogram Intersection Distance* is given by:

$$d_{hi}(x, y) = 1 - \frac{\sum_{i=1}^n \min(x_i, y_i)}{\sum_{i=1}^n \max(x_i, y_i)} \quad (18)$$

VII. EXPERIMENTS AND RESULTS

In this paper we propose a fast and effective method based on Angular Radial Transforms (ARTs) for the diagnosis of MCI individuals from AD and HC groups using structural MR brain images. The database of 210 MRI AD Neuroimaging Initiative is used for experiments. We considered 1 slice of all MR images in axial view and ARTs, OFMMs & ZMs were calculated as features for each MR brain image. An experimental study was conducted on the 1 slice of 210 ADNI MRI databases, which includes 70 AD patients, 70 MCI subjects, and 70 HCs. We chose 50 percent

of images (105 images) at random and used them in the training set (35 AD, 35 MCI and 35 HC) and rest 50 percent of images used as testing set. The author of (Gorji and Haddadnia, 2015) giving the classification rate higher as compared to our method because they have used 50% images for training purpose and only 25% images for testing phase. But in this paper we chose 50% of the images randomly for training purpose and rest 50% for testing phase, which increases the reliability of the detection of AD images.

Classification of AD and HC

Tables 1, 2 & 3 represent the classification of AD vs. HC images using ART, ZMs & OFMMs with different classifiers at different orders (order 5, 10 & 15) and from these details it is observed that the best results are obtained for AD/HC at order 15 (ART-87.143% & OFMMs-92.857%). It is also observed that the Angular radial transforms (order = repetition=10) with cosine measure classifier is giving the same accuracy as ZMs (order=15). The accuracy of AD/HC with ART, ZMs and OFMMs on different classifiers at different orders (order 5, 10 & 15) are plotted in figures 1, 2 & 3.

Classification of MCI and HC

Tables 4, 5 & 6 represent the classification of MCI vs. HC images using ART, ZMs & OFMMs with different classifiers at different orders (order 5, 10 & 15) and the best results were obtained for HC/MCI at order 10 (ART – 80%) and order 15 (OFMMs.-82.857%). The accuracy of HC/MCI with ART, ZMs and OFMMs on different classifiers at different orders (order 5, 10 & 15) are plotted in figures 4, 5 & 6.

Table 1: Classification of AD vs. HC images using ART, ZMs and OFMMs at order 5

| Classification Methods | Training Algorithms with Accuracy | | | |
|-------------------------------|-----------------------------------|----------|----------|-------------------------------|
| | ART | ZMs | OFMMs | ART |
| Cosine Measure (CM) | 87.143 % | 82.857 % | 81.429 % | Cosine Measure (CM) |
| Paper Similarity Measure (PS) | 82.857 % | 64.286 % | 80 % | Paper Similarity Measure (PS) |
| Euclidean Distance (ED) | 77.143 % | 68.571 % | 81.429 % | Euclidean Distance (ED) |
| Square Chord (SC) | 81.429 % | 75.714 % | 80 % | Square Chord (SC) |
| Chi Square (CS) | 82.857 % | 77.143 % | 78.571 % | Chi Square (CS) |
| Histogram Intersection (HI) | 72.857 % | 68.571 % | 77.143 % | Histogram Intersection (HI) |
| Extended Canberra (EC) | 82.857 % | 68.571 % | 80 % | Extended Canberra (EC) |

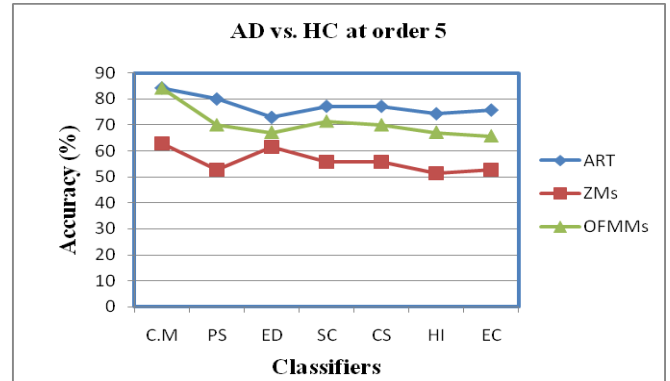


Fig 1: Classification accuracy of AD vs. HC with respect to order 5 of ART, ZMs and OFMMs

Table 2: Classification of AD vs. HC images using ART, ZMs and OFMMs at order 10

| Classification Methods | Training Algorithms with Accuracy | | |
|-------------------------------|-----------------------------------|----------|----------|
| | ART | ZMs | OFMMs |
| Cosine Measure (CM) | 84.286 % | 62.857 % | 84.286 % |
| Paper Similarity Measure (PS) | 80 % | 52.857 % | 70 % |
| Euclidean Distance (ED) | 72.857 % | 61.429 % | 67.143 % |
| Square Chord (SC) | 77.143 % | 55.714 % | 71.429 % |
| Chi Square (CS) | 77.143 % | 55.714 % | 70 % |
| Histogram Intersection (HI) | 74.286 % | 51.429 % | 67.143 % |
| Extended Canberra (EC) | 75.714 % | 52.857 % | 65.714 % |

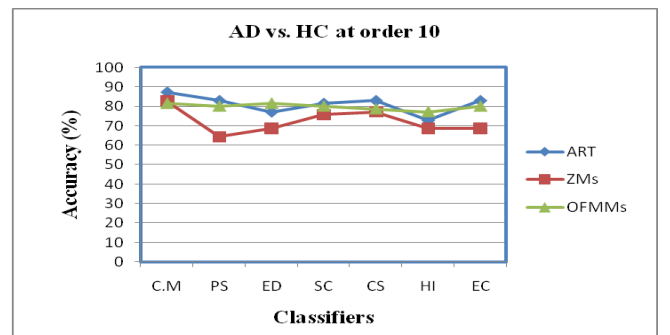


Fig 2: Classification accuracy of AD vs. HC with respect to order 10 of ART, ZMs and OFMMs.

Table 3: Classification of AD vs. HC images using ART, ZMs and OFMMs at order 15

| Classification Methods | Training Algorithms with Accuracy | | |
|-------------------------------|-----------------------------------|----------|----------|
| | ART | ART | ART |
| Cosine Measure (CM) | 87.143 % | 87.143 % | 92.857 % |
| Paper Similarity Measure (PS) | 77.143 % | 71.429 % | 81.429 % |
| Euclidean Distance (ED) | 80 % | 80 % | 77.143 % |
| Square Chord (SC) | 80 % | 80 % | 81.429 % |
| Chi Square (CS) | 80 % | 78.572 % | 84.286 % |
| Histogram Intersection (HI) | 80 % | 75.714 % | 81.429 % |
| Extended Canberra (EC) | 80 % | 74.286 % | 87.143 % |

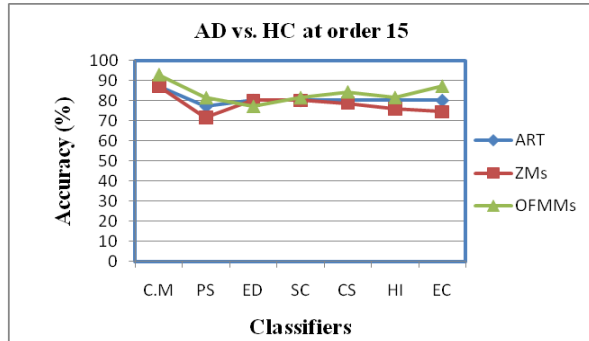


Fig 3: Classification accuracy of AD vs. HC with respect to order 15 of ART, ZMs and OFMMs.

Table 4: Classification of HC vs. MCI images using ART, ZMs and OFMMs at order 5

| Classification Methods | Training Algorithms with Accuracy | | |
|-------------------------------|-----------------------------------|----------|----------|
| | ART | ZMs | OFMMs |
| Cosine Measure (CM) | 80 % | 75.714 % | 77.143 % |
| Paper Similarity Measure (PS) | 75.714 % | 64.286 % | 72.857 % |
| Euclidean Distance (ED) | 60 % | 70 % | 67.143 % |
| Square Chord (SC) | 74.286 % | 64.286 % | 72.857 % |
| Chi Square (CS) | 72.857 % | 62.857 % | 72.857 % |
| Histogram Intersection (HI) | 65.714 % | 65.714 % | 72.857 % |
| Extended Canberra (EC) | 75.714 % | 61.429 % | 68.571 % |

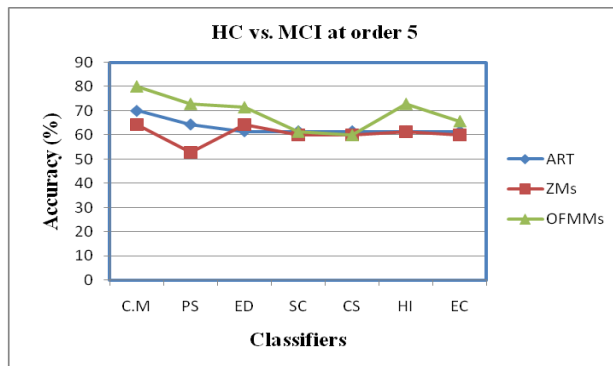


Fig 4: Classification accuracy of HC vs. MCI with respect to order 5 of ART, ZMs and OFMMs.

Table 5: Classification of HC vs. MCI images using ART, ZMs and OFMMs at order 10

| Classification Methods | Training Algorithms with Accuracy | | |
|-------------------------------|-----------------------------------|----------|----------|
| | ART | ZMs | OFMMs |
| Cosine Measure (CM) | 70% | 64.286 % | 80 % |
| Paper Similarity Measure (PS) | 64.286 % | 52.857 % | 72.857 % |
| Euclidean Distance (ED) | 61.429 % | 64.286 % | 71.429 % |
| Square Chord (SC) | 61.429 % | 60 % | 61.429 % |
| Chi Square (CS) | 61.429 % | 60 % | 60 % |
| Histogram Intersection (HI) | 61.429 % | 61.429 % | 72.857 % |
| Extended Canberra (EC) | 61.429 % | 60 % | 65.714 % |

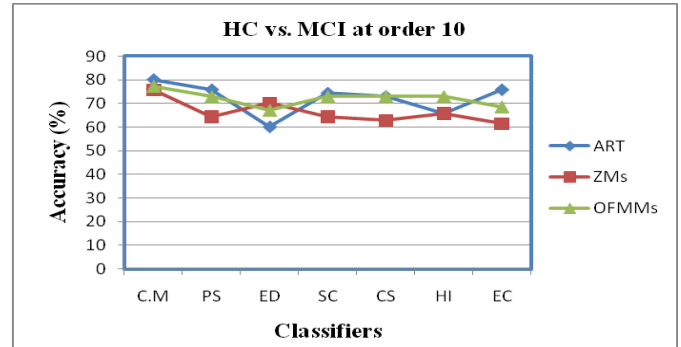


Fig 5: Classification accuracy of HC vs. MCI with respect to order 10 of ART, ZMs and OFMMs

Table 6: Classification of HC vs. MCI images using ART, ZMs and OFMMs at order 15

| Classification Methods | Training Algorithms with Accuracy | | |
|-------------------------------|-----------------------------------|----------|----------|
| | ART | ZMs | OFMMs |
| Cosine Measure (CM) | 74.286 % | 81.429 % | 82.857 % |
| Paper Similarity Measure (PS) | 64.286 % | 72.857 % | 71.429 % |
| Euclidean Distance (ED) | 64.286 % | 64.286 % | 68.571 % |
| Square Chord (SC) | 71.429 % | 62.857 % | 68.571 % |
| Chi Square (CS) | 68.571 % | 62.857 % | 67.143 % |
| Histogram Intersection (HI) | 67.143 % | 62.857 % | 70 % |
| Extended Canberra (EC) | 67.143 % | 65.714 % | 72.857 % |

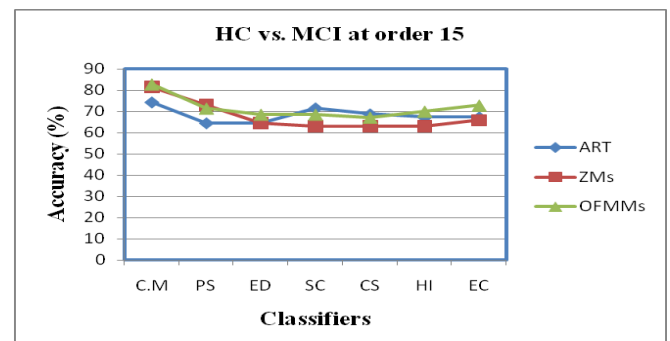


Fig 6: Classification accuracy of HC vs. MCI with respect to order 15 of ART, ZMs and OFMMs.

VIII. ANALYSIS AND DISCUSSION

We used fast and effective method based on rotation invariant descriptors to distinguish the patients with AD and MCI from normal participants (HC) and angular radial transform (ART) is one such rotation invariant descriptors. We also used Zernike moments (ZMs) and Orthogonal Fourier Mellin moments (OFMMs) to classify the information extracted from MR brain images of AD, MCI, and HC groups. The methods used not only for binary images but for gray level images also. We choose 50% of images at random for use in training the classifiers (35 AD,

35 MCI & 35 HC) & rest 50% of images used for testing phase. The method used is not only fast as compared to the existing available fastest methods but numerically stable too.

IX. CONCLUSION

Fast and effective technique for the computation of the ART and OFMMs are used in this paper to classify the information (features) extracted from MR brain images for early diagnosis of AD & classification between AD with HC and HC with MCI patients. The existing methods for extracting features from the structural MR brain images suffer from high time complexity and numerically instable at higher order of moments. The proposed approach uses recursive relations for the computation of sinusoidal radial and angular functions which are otherwise computation intensive. Further, the property of 8-way symmetry for the radial functions and 8-way symmetry/ anti-symmetry property for the angular functions reduce the number of computations from N^2 to $N(N+2)/8$ locations. It is observed that the proposed method is fast as compared to the existing available fastest methods. The proposed method is thus not only fast but numerically stable too. The fast computation of ART will, therefore, be very useful in many image processing and pattern recognition problems, such as template matching, character recognition etc. The obtained results have been obtained by increasing the testing images from 25% to 50%, which gives more reliability for early diagnosis of Alzheimer disease.

REFERENCES

- [1] R.S. Wilson, E. Segawa, P.A. Boyle, S.E. Anagnos, L.P. Hizek, D.A. Bennett, "The natural history of cognitive decline in Alzheimer's disease", *Psychol Aging*, Vol. 27, Issue 4, pp. 1008-1017, 2012.
- [2] W.W. Barker, C.A. Luis, A. Kashuba, M. Luis, D.G. Harwood, D. Loewenstein, C. Waters, P. Jimison, E. Shepherd, S. Sevush, N. Graff-Radford, D. Newland, M. Todd, B. Miller, M. Gold, K. Heilman, L. Doty, G. Pearl, D. Dickson, R. Duara, "Relative frequencies of Alzheimer's disease, Lewy body, vascular and frontotemporal dementia, and hippocampal sclerosis in the State of Florida Brain Bank", *Alzheimer Dis Assoc. Disorder*, Vol. 16, Issue 4, pp. 203-212, 2002.
- [3] M.M. Lopez, J. Ramirez, J.M. Gorriz, I. Alvarez, D. Salas-Gonzalez, F. Sequovia, R. Chaves, "SVM-based CAD system for early detection of the Alzheimer's disease using kernel PCA and LD", *Neuroscience*, Vol. 464, Issue 3, pp. 233-238, 2009.
- [4] R. Brookmeyer, S. Gray, C. Kaeas, "Projections of Alzheimer's disease in the 657 United States and the public health impact of delaying disease onset", *Am J Public Health*, Vol. 88, Issue 9, pp. 1337-1342, 1998.
- [5] N.C. Berchtold, C.W. Cotman, "Evolution in the conceptualization of dementia and Alzheimer's disease: Greco-Roman period to the 1960s", *Neurobiology of Aging*, Vol. 19, Issue 3, pp. 173-189, 1998.
- [6] S.C. Johnson, T.W. Schmitz, C.H. Moritz, M.E. Meyerand, H.A. Rowley, A.L. Alexander, K.W. Hansen, C.E. Gleason, C.M. Carlsson, M.L. Ries, S. Asthana, K. Chen, G.E. Alexander, "Activation of brain regions vulnerable to Alzheimer's disease: the effect of mild cognitive impairment", *Neurobiology of Aging*, Vol. 27, Issue 11, pp. 1604-1612, 2006.
- [7] P.M. Thompson, L.G. Apostolova, "Computational anatomical methods as applied to ageing and dementia", *Br J Radiol*, Vol. 80, Issue 2, pp. S78-S91, 2007.
- [8] J.L. Whitwell, S. Przybelski, S.D. Weigand, D.S. Knopman, B.F. Boeve, R.C. Petersen, C.R. Jack Jr., "3D maps from multiple MRI illustrate changing atrophy patterns as subject's progress from mild cognitive impairment to Alzheimer's disease", *Brain*, Vol. 130, Issue 7, pp. 1777-1786, 2007.
- [9] M. Grundman, R.C. Petersen, S.H. Ferris, "Mild cognitive impairment can be distinguished from Alzheimer's disease and normal aging for clinical trials", *Arch Neurol*, Vol. 61, Issue 1, pp. 59-66, 2004.
- [10] J. Bischof, A. Busse, M.C. Angermeyer, "Mild cognitive impairment-a review of prevalence, incidence and outcome according to current approaches", *Acta Psychiatr Scand*, Vol. 106, Issue 6, pp. 403-414, 2002.
- [11] T. Erkinjuntti, R. Sulkava, J. Palo, L. Ketonen, "White matter low attenuation on CT in Alzheimer's disease", *Arch Gerontol Geriatr*, Vol. 8, Issue 1, pp. 95-104, 1989.
- [12] H. Toyama, D. Ye, M. Ichise, "PET imaging of brain with the b-amyloid probe, [11C] 6-OH-BTA-1, in a transgenic mouse model of Alzheimer's disease", *Eur J Nucl Med Mol Imaging*, Vol. 32, Issue 5, pp. 593-600, 2005.
- [13] C. Davatzikos, Y. Fan, X. Wu, Dg. Shen, S.M. Resnick, "Detection of prodromal Alzheimer's disease via pattern classification of magnetic resonance imaging", *Neurobiology of Aging*, Vol. 29, Issue 4, pp. 514-523, 2008.
- [14] R. Chaves, J. Ramirez, J.M. Gorriz, M. Lopez, D. Salas-Gonzalez, I. Alvarez, F. Segovia, "SVM-based computer-aided diagnosis of the Alzheimer's disease using t-test NMSE feature selection with feature correlation weighting", *Neurosci. Lett.*, Vol. 461, Issue 3, pp. 293-297, 2009.
- [15] R. Cuingnet, E. Gerardin, J. Tessieras, G. Auzias, S. Lehericy, M.O. Habert, M. Chupin, H. Benali, O. Colliot, "Automatic classification of patients with Alzheimer's disease from structural MRI: a comparison of ten methods using the ADNI database", *Neuro Image*, Vol. 56, Issue 2, pp.766-781, 2011.
- [16] B. Magnin, L. Mesrob, S. Kinkingnehun, M. Pelegrini-Issac, O. Colliot, M. Sarazin, B. Dubois, S. Lehericy, H. Benali, "Support vector machine-based classification of Alzheimer's disease from whole-brain anatomical MRI", *Neuroradiology*, Vol. 51, Issue 2, pp. 73-83, 2009.
- [17] S. Kloppel, C.M. Stonnington, C. Chu, B. Draganski, R.I. Schajijl, J.D. Rohrer, N.C. Fox, C.R. Jack, J. Jr, Ashburner, R.S Frackowiak, "Automatic classification of MR scans in Alzheimer's disease", *Brain*, Vol. 131, Issue 3, pp. 681-689, 2008.
- [18] D. Shen, C.Y. Wee, D. Zhang, L. Zhou, P.T. Yap, "Machine Learning Techniques for AD/MCI Diagnosis and Prognosis", *Machine Learning in Healthcare Springer*, Vol. 56, pp. 147-179, 2012.
- [19] W. Yaping, "Kernel-based multi-task joint sparse classification for Alzheimer's disease" ISBI, 10th International Symposium on Biomedical Imaging, IEEE, 2013.
- [20] S.T. Yang, J.D. Lee, T.C. Chang, C.H. Huang, J.J. Wang, W.C. Hsu, H.L. Chan, Y.Y. Wai, K.Y. Li, "Discrimination between Alzheimer's disease and Mild Cognitive Impairment Using SOM and PSO-SVM" *Computational and mathematical methods in medicine*, 2013.
- [21] J. Escudero, J.P. Zalick, E. Ifeachor, "Machine Learning classification of MRI features of Alzheimer's disease and mild cognitive impairment subjects to reduce the sample size in clinical

- trials”, Engineering in Medicine and Biology Society, EMBC, Annual International Conference of the IEEE, 2011.
- [22] O. Colliot, G. Chetelat, M. Chupin, B. Desgranges, B. Maqnin, H. Benali, B. Dubois, L. Garnero, F. Eustache, S. Lehericy, “*Discrimination between Alzheimer Disease, Mild Cognitive Impairment, and Normal Aging by Using Automated Segmentation of the Hippocampus I*”, *Radiology*, Vol. 248 671, Issue 1, pp. 194–201, 2008.
- [23] C. Vinitha, M. Azath, “*Study on Image Authentication Techniques*”, *International Journal of Computer Sciences and Engineering*, Vol. 2, Issue 12, pp. 87-89, 2014.
- [24] H.T. Gorji, J. Haddadnia, “*A novel method for early diagnosis of Alzheimer's disease based on pseudo Zernike moment from structural MRP*”, *Neuroscience*, Vol. 305, pp. 361-371, 2015.
- [25] W. Kim, Y. Kim., “*A new region-based shape descriptor: the ART (Angular Radial Transform) descriptor*”, *ISO/IEC JTC1/SC29/WG11/M5472*, 2001.
- [26] M. Bober, “*MPEG-7 visual shape descriptors*”, *IEEE Transactions on Circuits and Systems for Video Technology*, Vol. 11, Issue 6, pp. 716–719, 2001.
- [27] A. Amanatiadis, V.G. Kaburlasos, A. Gasteratos, S.E.Papadakis, “*Evaluation of shape descriptors for shape-based image retrieval. Image Processing*”, *IET*, Vol. 5, Issue 5, pp. 493-499, 2011.
- [28] S.K. Hwang, W.Y. Kim, “*Fast and efficient method for computing ART*”, *IEEE Transactions Image Processing*, Vol. 15, Issue 1, pp. 112-117, 2006.
- [29] L. Kotoules, I. Andreadis, “*An efficient technique for the computation of ART*”, *IEEE Transactions on Circuits and Systems for Video Technology*, Vol. 18, Issue 5, pp. 682-686, 2008.
- [30] Y. Sheng, L. Shen, “*Orthogonal Fourier-Mellin moments for invariant pattern recognition*”, *J. Opt. Soc. Am.*, Vol. 11, Issue 6, pp. 1748-1757, 1994.
- [31] E. Walia, C. Singh, A. Goyal, “*On the fast computation of orthogonal Fourier- Mellin moments with improved numerical stability*”, *J Real- Time Image Proc.*, Vol. 7, pp. 247-256, 2012.
- [32] S.K. Hwang, W.Y. Kim, “*A novel approach to the fast computation of Zernike moments*”, *Pattern Recognition*, Vol. 39, pp. 2065–2076, 2006.
- [33] C. Singh, R. Upneja, “*Fast and accurate method for high order Zernike moments computation*”, *Applied Mathematics and Computation*, Vol. 218, pp. 7759-7773, 2012.
- [34] C. Singh, A. Kaur, “*Fast computation of Polar Harmonic Transforms*”, *Journal of Real-Time image processing*, Vol. 10, Issue 1, pp. 59-66, 2015.
- [35] G.A. Papakostas, Y.S. Boutalis, D.A. Karras, B.G. Mertzio, “*Fast numerically stable computation of orthogonal Fourier- Mellin moments*”, *IET Computer. Vis.*, Vol. 1, Issue 1, pp. 11-16, 2007.

Authors Profile

Rahul Upneja received undergraduate degree in Science in 2005 from Bikaner University, Bikaner, India, and post Graduate degree in Mathematics in 2007 from University of Rajasthan, Jaipur, India and Ph.D degree in Computer Science from Punjabi University, Patiala, India. He was an Assistant Professor in Department of Mathematics, Sri Guru Granth Sahib World University, Fatehgarh Sahib, India. He has already published 15 research papers in international journals and presented two papers in international conferences. His research interests include Image Processing and Numerical Analysis.



Ajay Prashar completed Master degree in mathematics in 2001, P.G.D.C.A in 2002 from D.A.V. College, Jalandhar, Punjab and M.Phil in 2007. He is pursuing his Ph.D. in mathematics. Dept. of Mathematics, Sri Guru Granth Sahib World University, Fatehgarh Sahib, India. Since 2003 he has been working as an Asst. Prof. in the Department of Mathematics (H.O.D) and Vice Principal in Trinity College Jalandhar, Punjab, India. He also served as Member of Board of studies (faculty of Sciences) Guru Nanak Dev University, Amritsar, Punjab, India. Currently he is pursuing Ph.D. from Sri Guru Granth Sahib World University, Fatehgarh Sahib, and Punjab. His current research interest is Image Processing.

